Non-Invasive Estimation of Atrial Fibrosis Location and Density

María Macarulla-Rodríguez[1], Jorge Sánchez[1], María S Guillem[1]

[1] ITACA Institute, Universitat Politècnica de València, Valencia, Spain

Abstract

Fibrosis can cause structural remodeling of cardiac tissue and increase the susceptibility to atrial fibrillation. The objective of this research is to determine the density and location of fibrosis by analyzing the P-wave morphology derived from 50 simulations of an atrial model with varying fibrosis characteristics. The density of fibrosis can be determined using sample entropy (SE) on the electrocardiogram (ECG) signal, with a tendency for entropy to increase with higher fibrosis density. The SE value was 1.16 times greater for cases with 5-7% fibrosis density compared to those with 0-1%. Additionally, the area under the curve of the ECG signal can be used to identify the location on the atria affected by fibrosis. This research provides essential insights into the relationship between P-wave morphology and fibrosis, paving the way for personalized treatment approaches based on fibrosis density and location.

1. Introduction

The presence of fibrosis in cardiac tissue is mainly a result of a regenerative process that involves the replacement of damaged myocardium with collagen. However, fibrosis alters atrial conduction, raising the predisposition to the most prevalent arrhythmia, atrial fibrillation (AF). Despite evidence implicating fibrosis in the perpetuation of AF, the basis of this association remains incompletely elucidated [1].

The location of fibrosis in the atria is a topic of debate. Studies have shown that AF patients are more likely to develop fibrosis in the posterior left atrium wall or pulmonary veins [2]. Research has predominantly focused on left atrium, resulting in limited exploration of right atrial fibrosis. Besides location, there is a high variability of fibrotic patterns and densities [1]. Although predicting the maintenance of AF based on fibrotic characteristics is challenging, categorizing fibrosis can aid in forecasting AF outcomes and developing personalized treatments.

Intracavitary mapping and delayed-enhancement magnetic resonance imaging are commonly used techniques to detect fibrosis in patients with cardiac diseases. However, these approaches have limitations [3], and computational modeling provides a promising alternative for further research on non invasive technologies that are not typically used to identify the location and density of fibrosis, such as electrocardiogram (ECG) or body surface potential mapping (BSPM). In study [4], the effect of fibrosis on the P-wave using metrics such as duration and amplitude is investigated to quantify fibrosis. Computer models also enable the creation of digital twins which can be used to simulate the impact of fibrosis on cardiac wave propagation and personalize treatment strategies. Kamali et al. [5] found that the models utilized were highly precise in predicting the outcomes of ablation procedures, exhibiting a favorable degree of correspondence with the results observed in clinical settings.

The present investigation involves the simulation of BSPMs obtained from six distinct patterns of fibrosis, together with eight locations of fibrotic areas on an atrial model. The main aim is to analyze the P-wave morphology in order to determine the density and location of fibrosis.

2. Materials and methods

2.1. Modeling methodology

In this research, an instance of an atrial statistical shape model [6] was used. The biatrial model was adapted to include anatomical features, such as specific anatomical and electrophysiological regions and the interatrial bridges. The atrial fiber orientation was defined following a rule-based method [7]. The volumetric biatria geometry average edge length was 550 μm. The human atrial electrophysiology was modeled by the mathematical formulation proposed by Skibsbye et al. [8]. The duration of the action potentials (APD_{90}) were adjusted to represent fifteen different electrophysiological regions [9]. Moreover, conduction velocities [10, 11] were tuned to obtain a total activation time of 115 ms for control case and 175 ms for the AF electrical remodeling case.

Additionally, fibrosis was added to the biatrial model to study the impact in the depolarization wavefront and its corresponding BSPM. Fibrosis was modeled using Perlin noise to create transmural fibrosis patterns that yield

realistic representations [12]. Eight locations were chosen to place the fibrosis: the posterior left atrial wall (pLAW), left inferior pulmonary vein (LIPV), left superior pulmonary vein (LSPV), right inferior pulmonary vein (RIPV), right superior pulmonary vein (RSPV), inferior cava vein (ICV), superior cava vein (SCV), and the right atrial septum (RAS). Fibrosis patterns were selected with the intention of including a wide range of distributions. These are: patchy and diffuse patterns, based on the distributions mentioned in [1], each with three variations in terms of density: 15%, 25%, and 40%. The density is quantified by dividing the number of fibrotic elements by the total number of elements within a given location. Fibrosis was modeled by elimination of mesh elements to represent the properties of fibrotic tissue. A total of 50 monodomain simulations were run using openCARP [13]. Stable limit cycle was reached by pacing at a basic cycle length of 1000 ms and 800 ms for the control case and AF remodeling, respectively. Furthermore, the BSPM was calculated assuming that the cardiac electric sources were immersed in an infinite conductive medium.

2.2. Analysis methodology

Signal analysis was performed using MATLAB (The MathWorks, Inc., USA, version 2023a). The sample entropy (SE) and area under the curve (AUC) of the ECG signals were computed to study how the variation of density and location of fibrosis affect the propagation of the electrical wave in sinus rhythm. SE was calculated using [14] to quantify the complexity of the signals due to fibrosis density, whereas the AUC was computed by integrating over the depolarization period to determine how the ECG signal amplitude was affected by the varying locations of fibrosis in the atria. The AUC calculation was conducted using electrodes arranged in a grid formation, as depicted in Figure 1. The grid comprises nine regions located on the anterior side of the torso (designated A1 to A9) and nine regions situated on the posterior side of the torso (P1 to P9), with an average of 27 electrodes per region. All the AUC measurements were subtracted with respect to the AF electrical remodeling (sAUC). A global normalization between 0 and 100 was performed to better identify the areas affected by the location of fibrosis. The average is computed over all the cases for each location of fibrosis on the atria.

3. Results

In Figure 2, the SE obtained from all the leads on the torso is shown. The fibrotic cases demonstrate higher SE resulting from signal fractionation (Figure 3). Specifically, the SE value for the electrical remodeled case is 1.18 times that of the control case. Additionally, the SE of the 5-7%

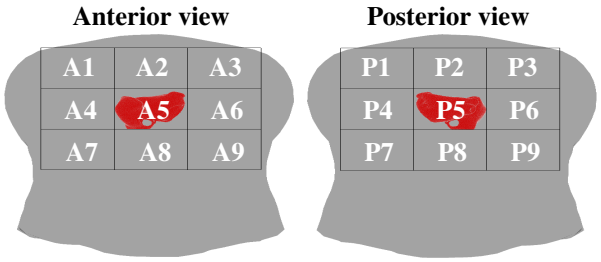

Figure 1. Electrode grid employed in AUC computation. Left: Anterior torso view, divided into regions A1 through A9. Right: Posterior torso view, divided into regions P1 through P9. Atria model is illustrated in red.

fibrosis density interval is 1.16 times higher than that of the 0-1%. The percentage is calculated by dividing the number of fibrosis-affected nodes by the total number of atrial nodes. It is observed that higher density corresponds to higher SE, indicating an association between the two variables. For a more detailed examination of the ECG signal, in Figure 3, leads II (a), and V3 (b) are shown for different simulations. Lead II was selected to detect propagation over the pLAW, where fibrosis is situated, while V3 was chosen due to its proximity to pLAW. It is noteworthy that a higher density of fibrosis results in more changes in amplitude of the signal due to the collisions of the electrical wave. As the density of fibrosis increases, non-conduction islands of tissue are formed, splitting the propagation wavefront and leading to subsequent collisions.

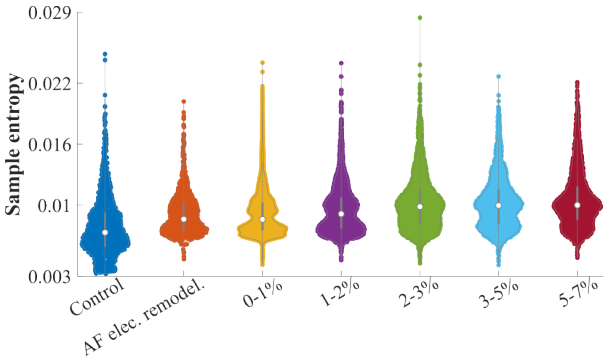

Figure 2. Violin plots of the SE. From left to right: control, AF electrical remodeling, and the fibrosis density intervals

The AUC values of the AF electrical remodeling case are represented in row a of Figure 4. Rows b and c correspond to the sAUC values of the cases of 25% patchy fibrosis on LIPV and 40% diffuse fibrosis on LSPV, respectively. The yellow regions correspond to higher values compared to the AF electrical remodeling case, while the blue regions indicate lower values of AUC. In the b row, lower values are present in A3 and A6, and greater values in regions P2 and P5. In contrast, in row c, there

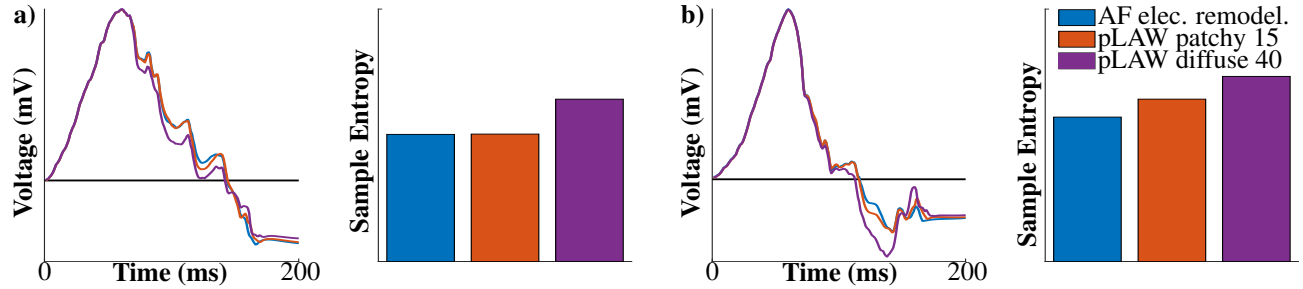

Figure 3. ECG signals and SE values for leads a) II, b) V3. AF electrical remodeling (blue), Fibrosis in pLAW: patchy 15% (red), diffuse 40% (purple).

are greater values in the anterior side of the torso, particularly in A2, and lower values in the posterior side of the torso, P4. Two distinct textures can be observed in the grid in rows b and c. This pattern particularity repeats for the 48 simulations, i.e., the texture changes when the fibrosis is located in different region, but variations in density or pattern of fibrosis only affect the amplitude of the values. It is worth noting that the two cases representing 15% fibrosis in the LIPV and LSPV exhibit the same texture as Figure 4, albeit with a decrease in the range of the value. Figure 5 contains a summary of all the textures belonging to the same location of fibrosis in the atria. Similar to Figure 4, the yellow regions denote AUC values greater than those of the AF electrical remodeling case, while the blue regions represent lower values. As mentioned before, simulations with fibrosis in the same regions exhibited similar textures. The density of fibrosis changed the sAUC amplitude values. Moreover, bigger areas affected by fibrosis such as the pLAW or RAS have higher sAUC range (from 0 to 100, and 33 to 81).

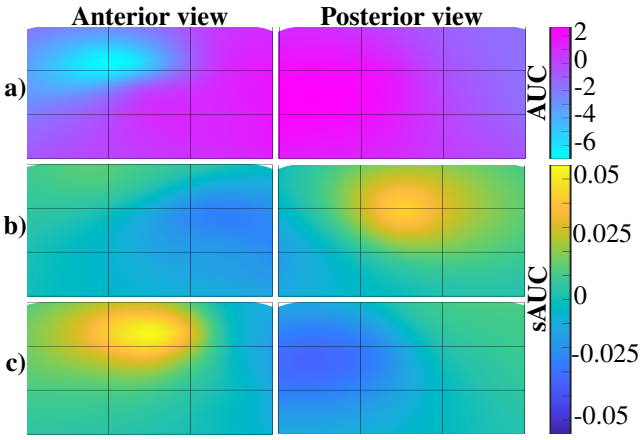

Figure 4. Anterior and posterior view of the torso (left and right columns). a) values for the AUC for the AF electrical remodeling case, b) and c) values for the sAUC for 25% patchy fibrosis in LIPV and 40% diffuse fibrosis in LSPV, respectively.

4. Discussion and conclusion

The aim of this research was to identify specific characteristics of P-wave morphology that could be used to differentiate between the location and density of fibrosis in the atria. The research demonstrated that fibrosis density can be determined using the SE, while the location of fibrosis can be identified using the AUC. The findings of Nagel et al. [4] demonstrated that the amplitude, duration and dispersion metrics of the signal were affected due to variation of fibrosis density, the duration being the most relevant. In our research, SE quantifies the extent of wave propagation disruptions caused by fibrosis density. Study [15] employs the P-wave integral maps to localize ectopic foci on regions of atrial models with fibrosis. Similarly, our research employs distinct textures of the sAUC metric to localize regions affected by fibrosis.

The identification of location and density can be employed in clinical settings to develop personalized treatment plans, as seen in [5], where they proposed ablation strategies to eliminate the recurrence AF cases. Similarly, our research findings indicate that fibrosis in various regions can be differentiated compared to cases with AF electrical remodeling. This suggests that in the clinical context, it might be feasible to compare a patient's signals to those of its digital twin with only electrical remodeling and consequently deduce the location and density of fibrosis. Acquiring information concerning the density of fibrosis can facilitate the decision-making of the treatment.

This research is limited by the use of one atrial model, which eliminates the variability that could be introduced by anatomical variability. It has been shown that variability in the atrial model causes changes in the morphology of the P-wave [4]. Future studies can incorporate multiple models to address this limitation. Moreover, additional patterns, densities, and locations of fibrosis can be incorporated to investigate whether the SE and sAUC are sufficient for the classification of fibrosis density and location.

In conclusion, this research demonstrates that SE can be a useful indicator of fibrosis density, and AUC can identify the location of fibrosis. The results presented are sig-

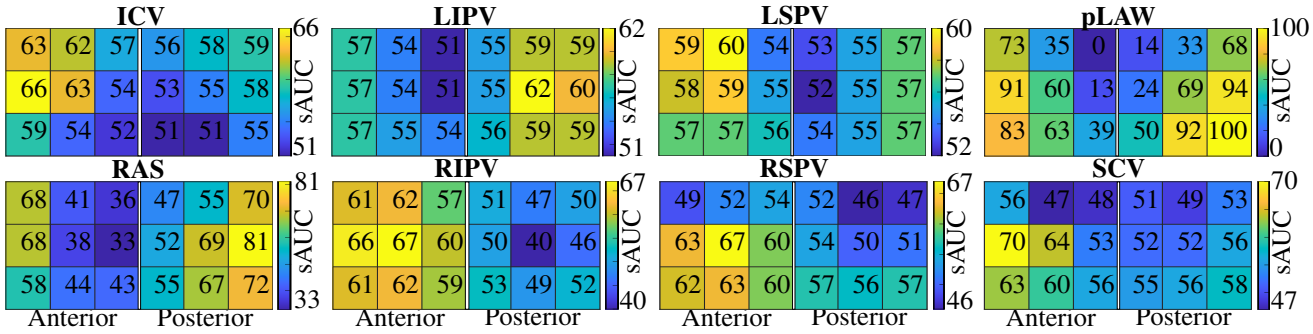

Figure 5. Normalized textures of sAUC for different anterior and posterior regions of the torso.

nificant in improving our understanding of the association between the P-wave morphology and fibrosis, and can potentially aid in the development of personalized treatments.

Acknowledgments

This project is part of the grant I+D+i PID2020-119364RB-I00 funded by the "Agencia Estatal de Investigación", and funded by the grant I+D+i PLEC2021-007614 by "European Union NextGenerationEU/PRTR".

References

[1] Xintarakou A, Tzeis S, Psarras S, Asvestas D, Vardas P. Atrial fibrosis as a dominant factor for the development of atrial fibrillation: facts and gaps. EP Europace 2020;22.

[2] Corradi D, Callegari S, Benussi S, Maestri R, Pastori P, Nascimbene S, Bosio S, Dorigo E, Grassani C, Rusconi R, et al. Myocyte changes and their left atrial distribution in patients with chronic atrial fibrillation related to mitral valve disease. Hum Pathol 2005;36.

[3] Quah JX, Dharmaprani D, Tiver K, Lahiri A, Hecker T, Perry R, Selvanayagam JB, Joseph MX, McGavigan A, Ganesan A. Atrial fibrosis and substrate based characterization in atrial fibrillation: time to move forwards. J Cardiovasc Electrophysiol 2021;32.

[4] Nagel C, Luongo G, Azzolin L, Schuler S, Dössel O, Loewe A. Non-invasive and quantitative estimation of left atrial fibrosis based on p waves of the 12-lead ecg—a large-scale computational study covering anatomical variability. J Clin Med 2021;10.

[5] Kamali R, Gillete K, Tate J, Abhyankar DA, Dosdall DJ, Plank G, Bunch TJ, Macleod RS, Ranjan R. Treatment planning for atrial fibrillation using patient-specific models showing the importance of fibrillatory-areas. Ann Biomed Eng 2022;51.

[6] Nagel C, Schuler S, Dössel O, Loewe A. A bi-atrial statistical shape model for large-scale in silico studies of human atria: model development and application to ecg simulations. MedIA 2021;74.

[7] Azzolin L, Eichenlaub M, Nagel C, Nairn D, Sanchez J, Unger L, Doessel O, Jadidi A, Loewe A. Augmenta: Patient-specific augmented atrial model generation tool. medRxiv 2022;.

[8] Skibsbye L, Jespersen T, Christ T, Maleckar MM, van den Brink J, Tavi P, Koivumäki JT. Refractoriness in human atria: Time and voltage dependence of sodium channel availability. JMCC 2016;101.

[9] Sánchez J. A Multiscale In Silico Study to Characterize the Atrial Electrical Activity of Patients With Atrial Fibrillation. Ph.D. thesis, Elektrotechnik und Informationstechnik des Karlsruher Instituts für Technologie, 2021.

[10] Ferrer A, Sebastián R, Sánchez-Quintana D, Rodriguez JF, Godoy EJ, Martinez L, Saiz J. Detailed anatomical and electrophysiological models of human atria and torso for the simulation of atrial activation. PloS one 2015;10.

[11] Van Schie MS, Heida A, Taverne YJ, Bogers AJ, de Groot NM. Identification of local atrial conduction heterogeneities using high-density conduction velocity estimation. EP Europace 2021;23.

[12] Sánchez J, Trenor B, Saiz J, Dössel O, Loewe A. Fibrotic remodeling during persistent atrial fibrillation: In silico investigation of the role of calcium for human atrial myofibroblast electrophysiology. Cells 2021;10.

[13] Plank* G, Loewe* A, Neic* A, Augustin C, Huang YLC, Gsell M, Karabelas E, Nothstein M, Sánchez J, Prassl A, Seemann* G, Vigmond* E. The openCARP simulation environment for cardiac electrophysiology. Comput Methods Programs Biomed 2021;208.

[14] Richman JS, Moorman JR. Physiological time-series analysis using approximate entropy and sample entropy. Am J Physiol Heart Circ Physiol AM J PHYSIOL HEART C 2000;278.

[15] Godoy EJ, Lozano M, García-Fernández I, Ferrer-Albero A, MacLeod R, Saiz J, Sebastian R. Atrial fibrosis hampers non-invasive localization of atrial ectopic foci from multi-electrode signals: a 3d simulation study. Front Physiol 2018;9.

Address for correspondence:

María Macarulla Rodríguez

ITACA. Edificio 8G acceso B. Universitat Politècnica de València. Camino de Vera s/n. 46022 Valencia, Spain.

mmacrod@itaca.upv.es